APPLICATION OF NEUTRON RADIOGRAPHY IN AEROSPACE INDUSTRY AND GEOLOGY

M. Bastuerk[1], M. Bichler[1], A. Dlouhy[2], H. Tatlisu[1], B. Zamani[1], M. Zawisky[1]
[1]Atominstitute of the Austrian Universities, Vienna, Austria
[2]Institute of Physics of Materials AS CR, Brno, Czech Republic

Abstract: The article describes the experimental procedures and results of radiographic and tomographic inspections in aircraft technology and geology. Turbine blade, made from TiAl alloys was investigated to reveal inhomogeneities that cannot be visualized by routine X-ray imaging. The alloy contains also about 1% boron to increase ductility and crack resistance. This makes neutron imaging a highly suitable technique because boron has a high neutron absorption cross section. Neutron and X-ray imaging can be used as complementary methods in the non-destructive material inspection, because the attenuation properties of materials depend on the radiation and its energy. Another application focused on the 3D visualization of internal structures of rock samples. The distribution of pore sizes and element distribution is demonstrated. Radiographic (thermal neutron and X-ray) and neutron tomographic investigations were carried out at the Atominstitut and Paul Scherrer Institute. Neutron inspections showed better contrast than X-ray due to the higher penetration ability for the inspections of thicker materials and their sensitivity to special isotopes.

Introduction: We present radiographic and tomographic inspections of a new turbine blade material [47Ti-48Al-2Cr-2Nb-1B (atom%)] and minerals distribution in rock samples. The main motivation of the TiAl investigations is to visualize interior defects and the distribution of boron. Radiography is a 2D imaging technique detecting the transmitted beam through the specimen on a screen, or in other terms, it is a visual representation of an object's interior. Conventional absorption radiography can be classified according to the used beam and its energy: cold-, thermal-, fast-neutron radiography, X-ray radiography, gamma-ray radiography e.t.c.. Tomography enables a 3D visualization of the internal structure of the object by reconstructing a set of radiography images, called projections, from different views; all 3D reconstructions in this article are based on the common FBP (Filtered Backprojection) method [1,2,3,4]. In some cases, comparison of different radiography methods like neutron and X-rays imaging facilitates the inspection of samples and provides more structural information. In addition, the comparison of different methods enables the determination of the most efficient method.

Excellent properties at elevated-temperatures and low density make the titanium aluminide (TiAl) an attractive candidate for both, engine and airframe applications, particularly in the aerospace industry. Among TiAl-based materials, gamma TiAl is the most promising alternative. It reduces the weight of aircraft engines by virtue of its low density and high temperature capability, and has advantages in stiffness, fire and corrosion resistance. The performance in the transitional state between the turbine at rest and a particular speed of rotation is important in order to improve the efficiency. The use of light materials such as gamma TiAl alloy for the turbine blades is desirable in reducing the transitional time and inertia of the turbine rotors. The characteristics of aircraft engines affect the revenue, as well as the total weight reduction [5,6,7]. The addition of the elements Cr and B increases the room temperature ductility, and Nb the oxidation resistance. Boron forms TiB_2 borides, which improve the stability of the grain structures during various thermo-mechanical treatments. The mechanism of ductilization is unclear; it is assumed that the boron segregates into grain boundaries, enhancing thus the cohesive strength of the boundary [8,9]. Hence, prototype TiAl turbine blades containing 1atom% B were investigated. In addition to the material characteristics, aero-engine applications require careful processing route involving casting, forging, machining or joining to produce complex geometries. The final mechanical properties of the alloy depend strongly on the machining [10,11,12]. The present work aimed at visualizing inner cracks or defects of the test sample resulting from the manufacturing process.

Another application of neutron radiography (NR) and neutron tomography (NT) presented in this work helps to visualize the distribution of minerals in rocks. Size and distribution of minerals as well as the internal structure yield valuable information for petrologic research and for the applicability as construction material. Examples are the distribution of mica in pumice and in granite, Fe-spinel in serpentinite and silica gel in artificially impregnated calcareous sandstone. Silica gel (SiO_2) as a moisture adsorbent is an important material in industry [13]. The investigation of rock samples with neutron imaging was carried out at the Atominstitut in Vienna (ATI) and the Paul Scherrer Institute (PSI) in Villigen, the X-ray applications were done at the Atominstitut. ATI has two NR beam ports (NR-I, NR-II); NR-I based on neutron converter/X-rays film is used for radiographic inspections of large objects, and NR-II having a digital detection system (neutron sensitive scintillator/digital CCD camera) is for radiographic and tomographic applications [1,3]. The comparison of the beam characteristics of both NR working stations with NEUTRA-PSI is given in table-1.

Table-1: Characteristics of the NR beam ports at ATI and PSI.

	NR-I (ATI)	**NR-II (ATI)**	**NEUTRA (PSI)**
Neutron flux ($cm^{-2}.s^{-1}$)	$3x10^5$	$1.3x10^5$	$3x10^6$
Collimation ratio	50	~ 130	550
Cd ratio	3	20	100
Beam diameter (cm)	40	9	40
Detection system	Gd converter/ X-ray film	0.4 mm thick ZnS(Ag)-^{6}LiF scintillator/CCD camera (512x512 pixels)	0.25 mm thick ZnSAg-^{6}LiF scintillator/CCD camera (1024x1024 pixels)

Results and Discussion: At the beginning, neutron and X-ray radiography measurements of the TiAl test sample developed by the Institute of Physics of Materials in Czech Republic were performed at Atominstitut in order to find the most efficient method. The aim was to visualize manufacturing defects for quality control. According to the radiographic images shown in Fig. 1, X-ray image taken at 55 kV, 20 mA for 60 s exposure time gave insufficient information about the TiAl turbine blade; the thickness of turbine blade varies from 2 mm to ~ 2 cm. As a result, an increase in energy and density of X-rays beam caused disappearance of the image contrast in thinner parts of the sample. On the other hand, the sample is quite transparent for neutrons (left side in Fig. 1) taken with a digital CCD camera for 40 s exposure time. Bright pixels represent the high beam transmission (low absorption) for the radiography images, while for the 3D reconstructed tomography images bright pixels correspond to the high beam attenuation (high absorption) by the material.

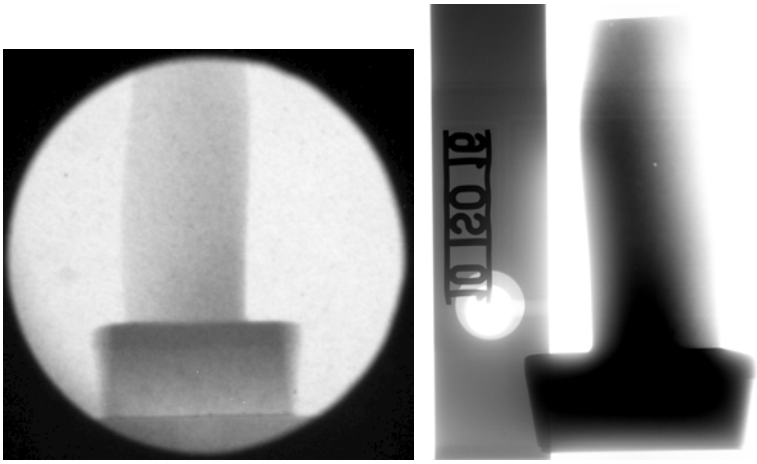

Fig. 1: Radiographic inspections of TiAl turbine blade; left side by neutron radiography and right side by x-ray imaging.

Even though the neutron radiography image shows that the TiAl sample is homogeneous and free of defects, neutron tomography was applied in order to get more information about the sample's interior. For 3D image reconstruction, 200 NR projections were taken with 40 s exposure time per projection with 0.9° angular steps from different views. Enhancing the image contrast and cutting the 3D images slice by slice with the help of the rendering software (VolumeGraphics), the inhomogeneities and defects within the sample were visualized in Fig. 2 (marked parts). The inhomogeneity increases with the thickness of the turbine blade. In addition, some defects like cracks that might form during the material processing (casting, forging, machining and joining) could be visualized as marked in the fourth image in Fig. 2. Any inhomogeneity respective to the distribution of boron (1 atom%) could not be visualized with the spatial resolution of 300 μm.

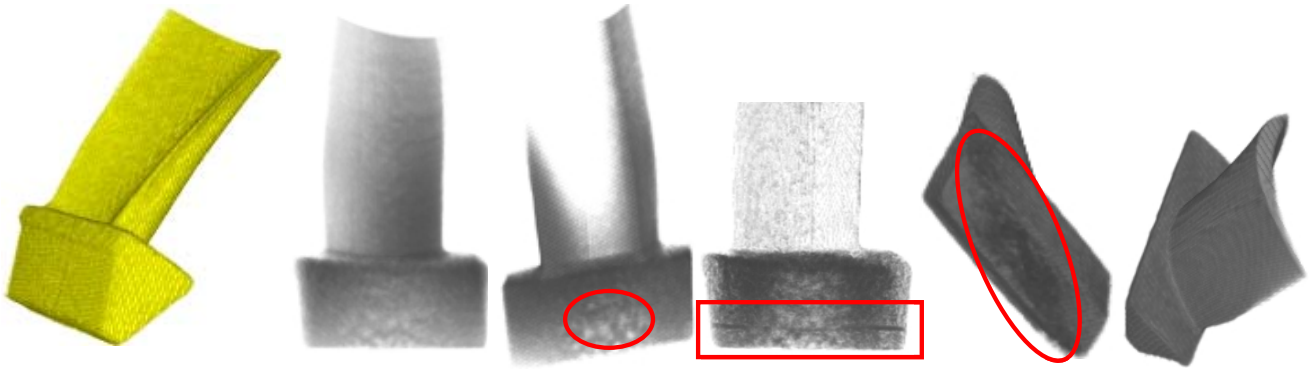

Fig. 2: 3D reconstructed NT images of the TiAl turbine blade with different opacity levels; the inhomogeneous parts were marked, first and last images (from the left) are with full opacity, third and fifth images with enhanced contrast. The fourth one (from left) with high transparency shows a crack in the middle of the sample.

The distribution of minerals in rock samples is shown in Fig.s 3-6. The NT measurements were performed at the PSI with ~ 100 μm spatial resolution. The first one is pumice, a highly vesicular volcanic rock, mainly consisting of silicate glass. The mineral biotite (black mica) contains significantly more iron and hydrogen than the surrounding glass and is well shown due to the higher neutron absorption cross sections of these elements (Fig. 3). To facilitate the visualization of biotite, a segmentation process was applied; the yellow colored parts indicate biotite while the gray colored parts are silicate glass. Furthermore, one of the segments (in this case glass) was cut

to highlight the other segment. A comparable picture results from NT of granite (Fig. 4). The mineral biotite is shown while the other mineral components such as quartz and feldspar show properties similar to that of the pumice glass.

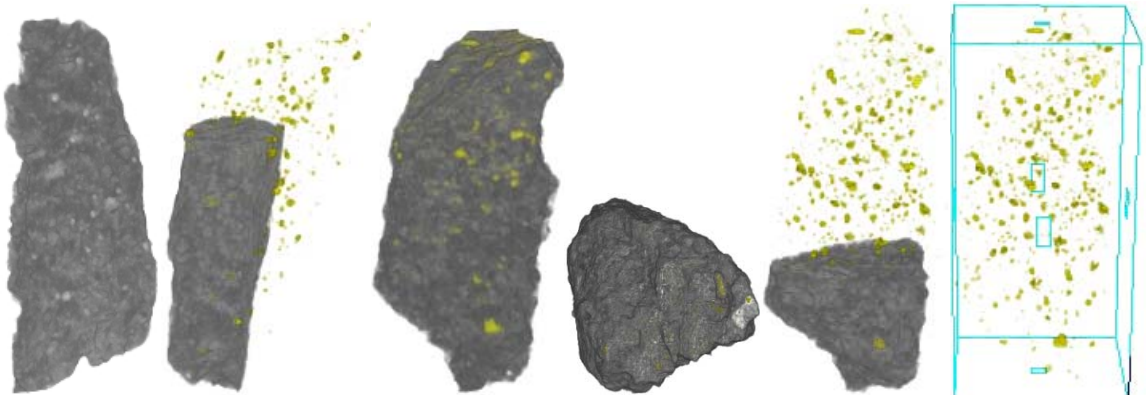

Fig. 3: 3D reconstructed NT images of pumice from different views (240 projections taken with 10 seconds exposure time each); first and fourth images (from left side) taken from different views are without segmentation, the further images are with two segmentations indicating pumice (grey) and biotite (yellow, the pumice segment was cut slice by slice to show only the biotite segment in the last image).

Fig. 4a shows the radiography images of neutrons and X-rays respectively. Biotite is seen in both radiographies due to its Fe and hydrogen content. Therefore, no specific difference can be visualized between both radiography images in Fig. 5a. Fig. 5b shows the distribution of biotite within the granite step by step from left to right.

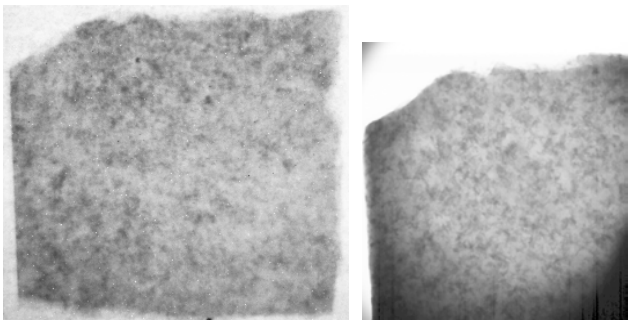

a)

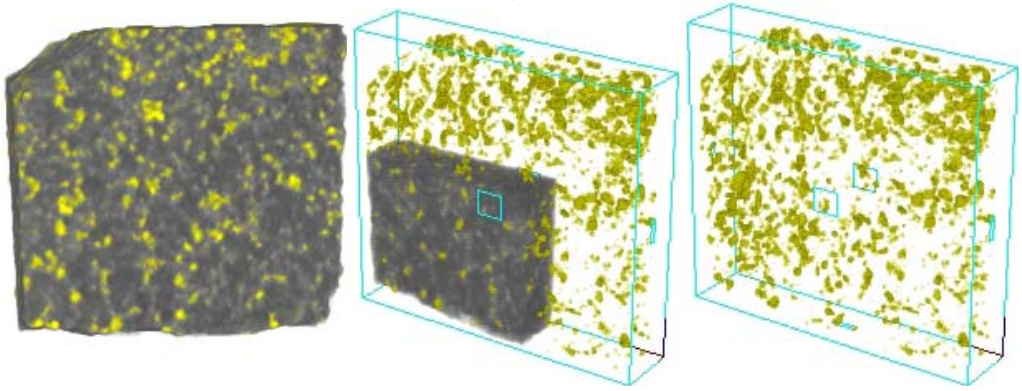

b)

Fig. 4: 2D and 3D reconstructed images of the granite (fine grained) rock sample showing mica Biotite mineral distribution; a) neutron radiography (left), and x-ray radiography (right) showing one part of the granite sample taken at 40 kV, 12 mA for 5 seconds at ATI, b) 3D reconstructed NT images (from 240 projections taken at PSI with 15 seconds per projection) showing Biotite mineral in yellow segments.

Silica gel is used for the preservation of natural stone surfaces of historical buildings to prevent progressive weathering. The surfaces are impregnated with a solution of tetraethoxysilane, which decomposes by precipitation of silicagel and evaporation of ethanol. Silicagel contains a certain amount of water, which offers good properties for a 3D imaging by NT. The quality of an impregnation depends on the distribution of the agent throughout the (usually porous) rock structure and can therefore be checked by NT. Additionally, the quantity necessary can be optimized economically. As an example, an impregnated sample of tertiary calcareous sandstone (St. Margarethen, Austria) was used. The material has been prepared during a research cooperation for the restoration of St. Stephen's cathedral in Vienna, Austria. The measurements performed at ATI improved our understanding of the water adsorption and desorption by silica gel and other water absorbing components like clay minerals. Fig. 5 shows the distribution of silica gel and water within the inspected sandstone sample before and after a drying process at 110 °C over 24 hours. The sample was bonded on a sample holder with an adhesive resulting in absorption maxima at the corners. In this manner, the adhesive on the corners containing hydrogen was taken as a comparison point in the segmentation of the silica gel and adhesive from the rock sample, as seen in Fig. 5a. After heating through 24 hours, the sample was measured again in order to analyze the water desorption. As shown in Fig. 4b, the water content within the impregnated rock sample has been reduced, but a certain amount of water remained adsorbed tothe silicagel.

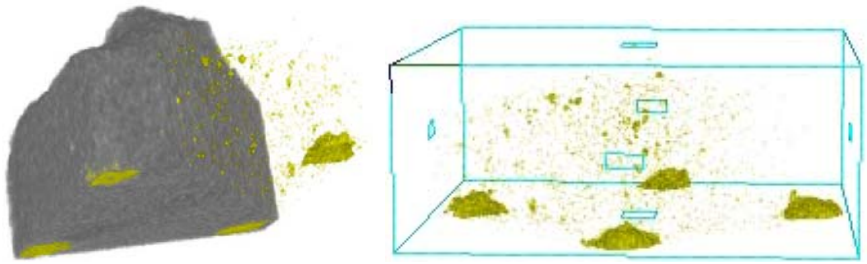

a)

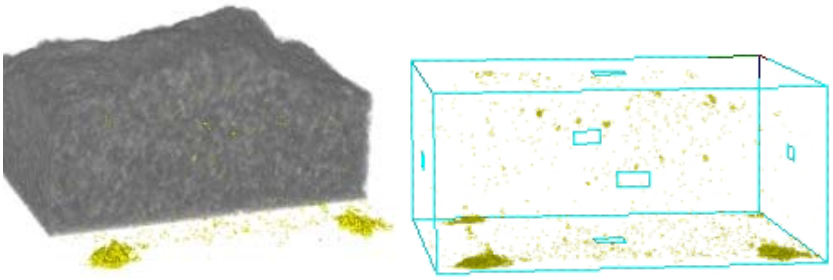

b)

Fig. 5: NT images (from 200 projections taken at ATI with 35 seconds per projection) of the silica gel / water distribution within the sandstone; a) before the drying process, b) after heating to 110 °C for 24 hours; gray segments showing the sandstone and yellow segments silica gel or other hydrogen containing minerals.

Finally, we present the results of a serpentinite rock sample measurement with X-ray and neutron imaging. Serpentine ($(Mg,Fe)_3Si_2O_5(OH)_4$) is a family of silicate minerals rich in magnesium and water, and rocks made up of serpentine minerals are called serpentinite [14,15]. Additionally to serpentine, the sample contains the iron-spinel phase magnetite (Fe_3O_4) and some accessory Ca-carbonate. Thermal neutron and X-ray radiography measurements were carried out to compare the observed minerals within the serpentinite rock sample as shown in Fig. 6a. The comparison between the NR and X-ray images (particularly marked parts on the images) gives an idea about the visualized elements within the sample. The pictures show the intensive attenuation of neutrons due to the high crystal water content in serpentine in contrast to the X-ray radiography. Because of the insufficient beam cross section, X-rays images were performed at 40 kV, 10 mA for 5 seconds from the upper and lower part of the sample, separately (middle and right image in Fig. 6a). For the NT measurement, a segmentation process between minerals is not possible owing to the intensive intergrowth of the minerals.

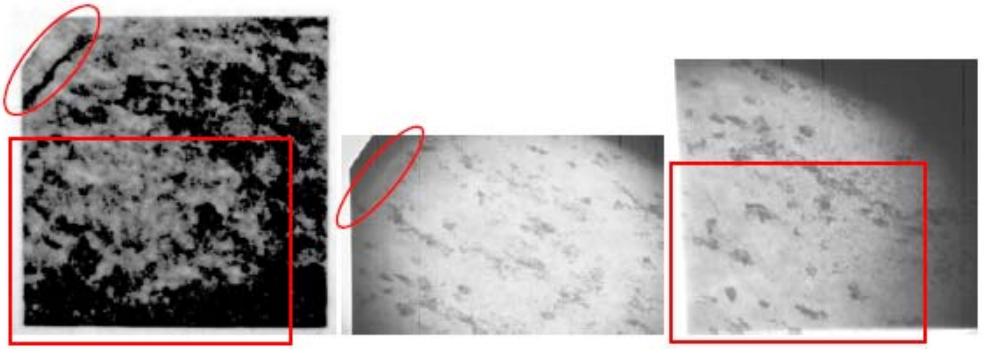

a)

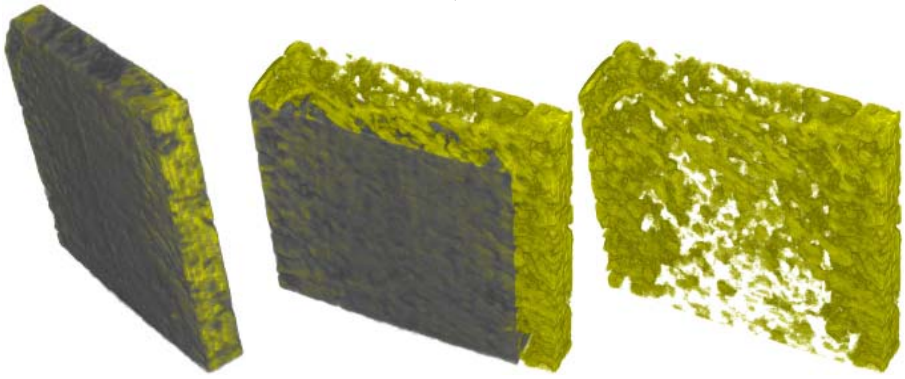

b)

Fig. 6: Imaging of serpentinite rock sample; a) thermal neutron radiography (left) and X-ray radiography images (middle image showing left upper edge and right image showing left bottom edge of the sample), b) 3D reconstructed NT images (from 240 projections taken at PSI with 15 s per projection) of hydrogen distribution from different views with different cutting slices; the yellow segment shows the distribution of the highest neutron attenuation (mainly due to the mineral serpentine)

Conclusions: We presented applications of thermal neutron radiography and tomography in aerospace and geology. The boron concentration in the TiAl turbine blade is distributed homogeneously up to the detection limit of 300 μm spatial resolution. The heterogeneity increases with the thickness of the TiAl component. Some interior defects like edge cracks could be observed at the transition from thinner to thicker parts, which are probably caused by the manufacturing process. In the inspections of rock samples, the efficacy of a silica gel

impregnation was presented with the help of the strong neutron attenuation property of hydrogen. Besides the visualization of silica gel distribution within the rock samples, water adsorption and desorption properties could be determined with systematic investigations. On this account, the inspections of natural stone based construction material will be continued focusing on the quantitative analysis of water content. The minerals, which contain one of the strong neutron attenuators like H, B, Fe etc., can easily be determined by neutron imaging. The distribution of the minerals biotite and serpentine was visualized without any problem.

Acknowledgement: The authors would like to thank Peter Wobrauschek for his helps during the X-ray radiography inspections, Peter Vontobel and Stefan Hartmann for the technical support during the experiments at NEUTRA-PSI. This work was financially supported by the EURATOM-ÖAW, UT4-Underlying Technology project.

References:

[1] M. Bastürk, Material inspections with low energy neutrons and 3D image reconstruction, Dissertation at TU-Vienna, Austria, 2003.
[2] M. Zawisky , M. Bastürk , J. Rehacek and Z. Hradil, Neutron tomographic investigations of boron-alloyed steels, Journal of Nuclear Materials 327, Issues 2-3, Pages 188-193, 2004.
[3] S. Koerner, Digital image processing in neutron radiography, Doctoral thesis, TU-Vienna 2000.
[4] S. Koerner, B. Schillinger, P. Vontobel, H. Rauch. A neutron tomography facility at a low power research reactor, Nuclear Instr. and Methods in Physics Research A 471 (2001) 69-74.
[5] David Trinh, Matthias Müller, Aluminides, 4H1609 Functional Materials, Project report, KTH 2002.
[6] S.C. Huang, J.C. Chesnutt, Gamma TiAl and its Alloys, Intermetallic Compounds, vol. 2, John Wiley & Sons, p. 73. 1994.
[7] T. Noda, Application of cast gamma TiAl for automobiles, Intermetallics 6, pp. 709-713, 1998.
[8] C.M. Austin, Current status of gamma Ti aluminides for aeurospace applications, Current Opinion in Solid State & Material Science 4, pp. 239-242, 1999.
[9] Donald E. Larsen, Jr., Status of investment cast gamma titanium aluminides in the USA, Material Science & Engineering A213, pp. 128-133, 1996.
[10] T. Tetsui, S. Ono, Endurance and composition and microstructure effects on endurance of TiAl used in turbochargers, Intermetallics 7, pp. 689-697, 1999.
[11] M. H. Loretto et al., The influence of composition and processing on the structure and properties of TiAl-based alloys, Intermetallics 6, pp. 663-666, 1998.
[12] A.-L. Gloanec et al., Fatigue crack growth behaviour of a gamma-titanium-aluminide alloy prepared by casting and powder metallurgy, Scripta Materialia 49, pp. 825-830, 2003.
[13] Steven Weintraub, Demystifying silica gel, Humidity control with silica gel, silica gel reconditioning, technical papers, Art Preservation Services, http://www.apsnyc.com/.
[14] http://www.webmineral.com/.
[15] http://www.mindat.com/.